



PREDICTING RESPONSE OF NON-LINEAR HIGH DAMPING RUBBER ISOLATION SYSTEMS

H.R. AHMADI, K.N.G. FULLER and A.H. MUHR

Malaysian Rubber Producers' Research Association, Brickendonbury,
Hertford SG13 8NL, UK

ABSTRACT

A theoretical study assessing how the choice of model affects the predicted response of a rigid structure mounted on high damping rubber isolators is presented. A non-linear hysteretic model is introduced as a benchmark for comparison with linear models employing three different methods of linearizing the observed dynamic properties. The linear model with modulus and damping calculated using the secant method gives predictions closest to those of the non-linear model. At design level earthquakes the differences ranged up to about 13%, but for more severe inputs the discrepancies can be substantially greater. The linear prediction often underestimates the response to ground motions.

KEYWORDS

Response prediction; non-linear analysis; linear analysis; hysteretic damping model; high damping natural rubber; base-isolation; seismic isolation; isolators; dynamic properties.

INTRODUCTION

Structures in several countries have been protected from the effects of horizontal seismic ground motion by mounting them on high damping natural rubber (HDNR) bearings. This technique is a simple and economical means of providing seismic isolation. The purpose of this paper is to discuss the dynamic stress-strain characteristics of HDNR, with a view to modelling the seismic response of a structure isolated on HDNR bearings. Under vertical loads much less than the buckling load and for moderate horizontal deformations, the horizontal load-deflection behaviour may be calculated quite accurately from the stress-strain properties of the rubber in simple shear. Additional contributions to damping may sometimes arise from yielding of the internal reinforcing shims but this paper will consider the damping to arise from the HDNR alone.

In the rubber industry it is conventional to use a linear viscoelastic model for the dynamic properties of rubber (eg. ISO 2856). For unfilled rubbers this representation is quite realistic, but the hysteresis loops for filled rubbers such as HDNR are distorted, and those corresponding to a lower amplitude have a greater slope (Fig.1). Nevertheless, a dynamic modulus G_{dyn} and loss angle δ may be calculated from the loop for a given strain amplitude, producing strain-dependent values of G_{dyn} and $\tan\delta$. There is interest in quantifying the differences between the response of HDNR isolation systems predicted using such linearised properties and those using a bi-linear or non-linear representation. Skinner *et al* (1993), who were concerned with lead-plug rubber isolators,

compared predictions of the response for bi-linear representations with those of the equivalent linear ones. They found that the equivalent linear (Kelvin) model may be used to make rough predictions of the peak seismic responses of the first mode, the uncertainty in prediction of peak bearing deflection (from this source) being of the order of $\pm 15\%$ for the El Centro accelerogram.

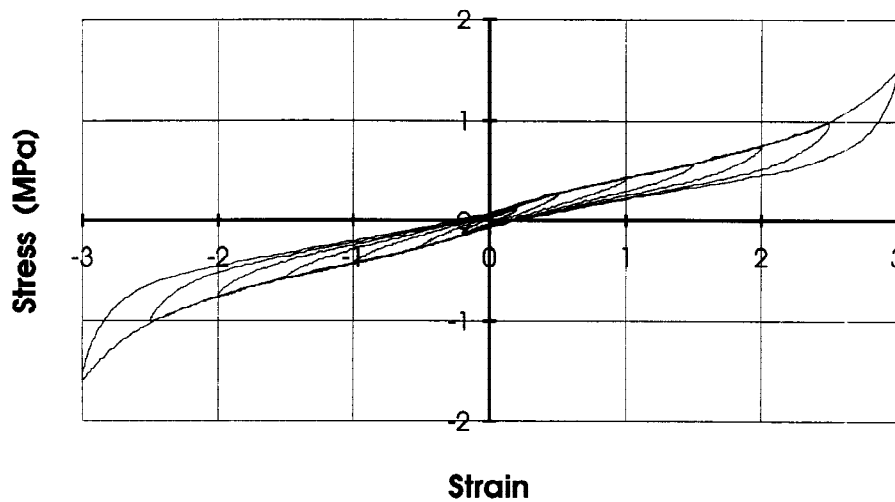


Fig.1. Shear stress-strain loops for a soft HDNR tested sinusoidally at 0.5Hz at successively larger amplitudes from 20% to 300%. Six 300% scragging cycles followed by 1 minute pause were interposed between each strain test.

If a linear representation is used, a choice of linearisation method has to be made. Three different methods are considered here. In addition, the rubber shear strain amplitude at which the linearised parameters are calculated must be chosen. Usually the strain corresponding to the maximum displacement amplitude is specified; an iteration procedure is adopted to ensure the predicted response is consistent with the specified strain. Alternatively the linearised properties may be calculated for an average of the strain throughout the response (Fuller *et al*, 1991). The optimum choice of strain may depend on the main parameter of interest (eg. peak bearing displacement or peak acceleration) in the response. The choice may not be very important provided the maximum strain falls in the regime of weak amplitude dependence of G_{dyn} . The rubber strain corresponding to the design earthquake is commonly chosen to be in this region.

This paper compares numerically predicted responses of SDOF oscillators to earthquake excitations using Kelvin, bi-linear and non-linear hysteretic models for HDNR. The last model, presented in some detail, is devised to describe the behaviour at any amplitude and may therefore be used without the need for iteration to determine appropriate parameters.

MODELS FOR DYNAMIC PROPERTIES OF HDNR

A non-linear hysteretic model

The model, a refinement of the multi-linear model described by Ahmadi *et al* (1995), (see Fig.2) is based on the observed stress-strain loop of the compound tested in simple shear at a frequency of 0.5Hz and at the largest strain amplitude of interest. During cycling at that amplitude the upper half of the model hysteresis loop partly follows the curve τ_1 and the lower half the curve τ_2 . The two curves are assumed to possess a centre of symmetry about the origin, and are constructed from the observed hysteresis loops. The method of calculating the stress response to an arbitrary strain history is described below.

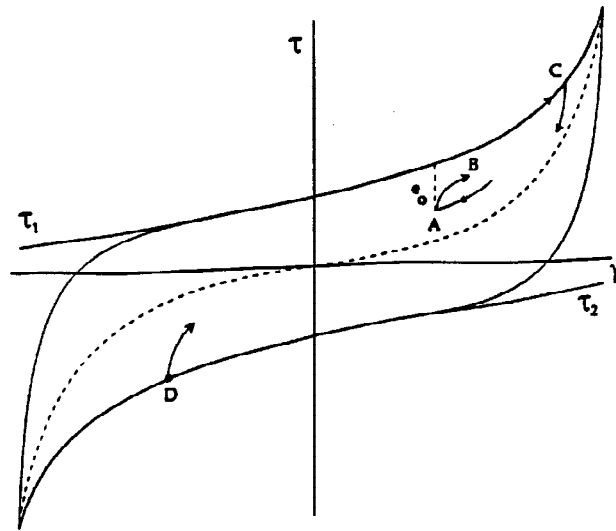


Fig.2. Non-linear hysteretic model for filled rubber

During a general deflection-time history, a strain reversal may occur at any point such as A within the model loop. For the case in which the strain changes from decreasing to increasing (here the sign attached to the strain has to be taken into account) i.e. for loading, the amount e_0 by which the stress at A falls below τ_1 (extrapolated to lower strains if necessary) is considered. The loading path B is defined by the relation:-

$$\frac{d\tau}{d\gamma} = \frac{d\tau_1}{d\gamma} \left(1 + K_1 \frac{e}{e_0} \right) + L \frac{e}{e_0} \quad \text{where } L = K_2 \left| \frac{d\tau_1}{d\gamma} - \frac{d\tau_2}{d\gamma} \right| \quad (1)$$

and e is the amount by which the stress at strain γ differs from that given by the curve τ_1 ; K_1 and K_2 are constants. If after reversing the direction of deformation the strain is decreasing, the subscripts 1 and 2 are reversed in eq.(1), and e_0 and e are measured from the curve τ_2 . Each strain reversal defines a new starting position. The retraction parts of the model loop - the dashed lines in Fig.2 - are derived from eq.(1).

Figure 1 shows the experimental stress-strain loops for a soft high damping natural rubber (HDNR) compound. The loop for the largest strain amplitude (i.e. 300%) was used to construct curve τ_1 (see Fig.3), the part from point B to the maximum strain amplitude being the corresponding section of τ_1 . The position of point B is

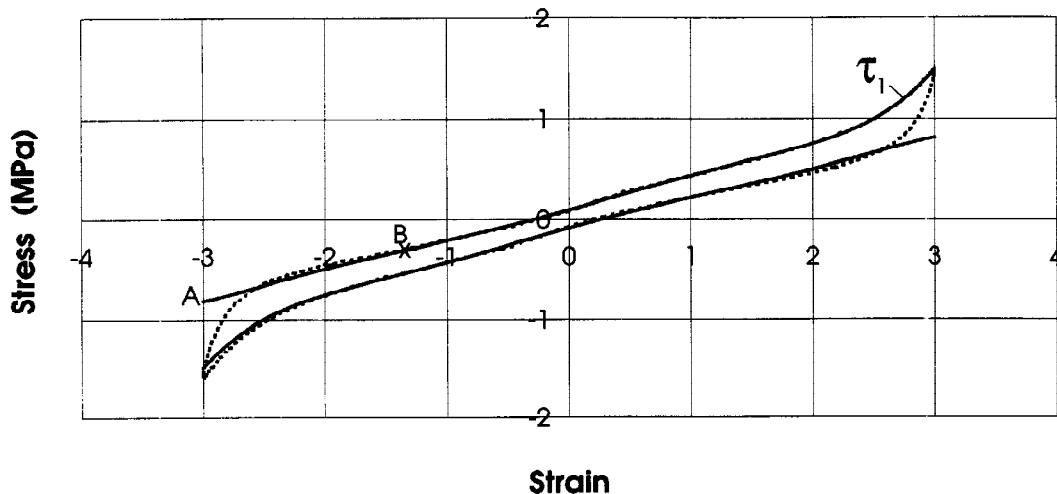


Fig. 3. Hysteresis loop at 300% strain used to generate τ_1 curve for the non-linear hysteretic model

chosen so that the waisting in the centre of the hysteresis loop is followed by the curve τ_1 , otherwise the model will overestimate the loss factor. The section AB of τ_1 is a straight line. Varying its slope provides fine adjustment enabling the model loops to give the best representation of the strain amplitude dependence of the loss factor. The parameters with the major influence on the magnitude of the loss factor are K_1 and K_2 . These are adjusted to give an area for the model loops as close as possible to that of the observed loops. The lower strain amplitude loops ($\gamma_{\max} < 150\%$), for which there is no significant upturn, are influenced primarily by K_1 and the higher strain ones by K_2 . For the loops shown in Fig.2, the fitted values for K_1 and K_2 are 0.9 and 4.5 respectively. The experimental loops and those predicted by the model are shown for 100 and 300% strain amplitudes in Fig.4. The predicted loops are seen to correspond quite well with the observations.

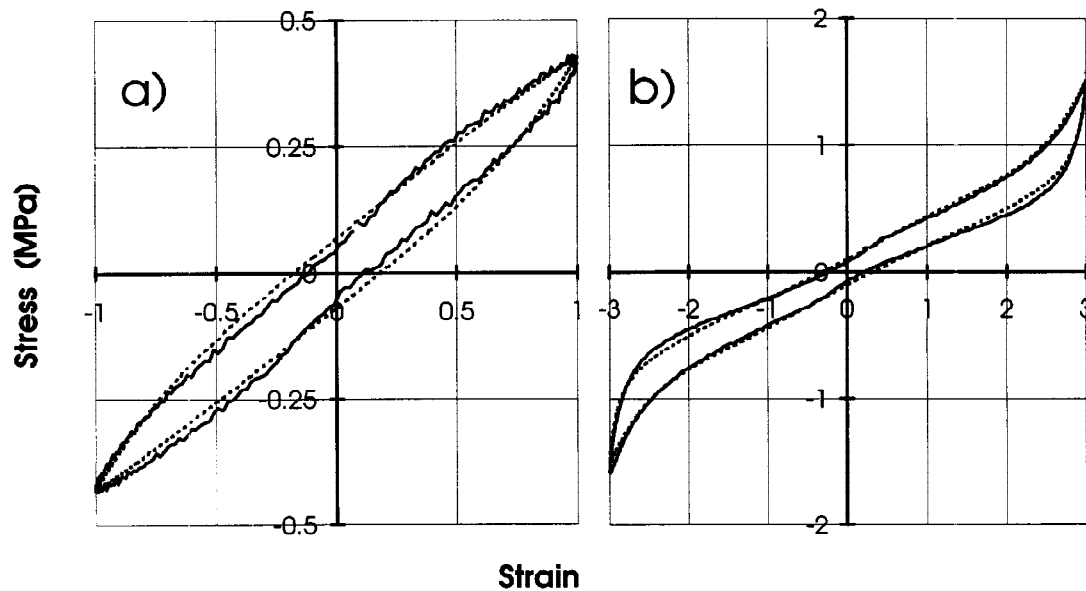


Fig.4 The experimental hysteresis loops (—) for (a) 100% and (b) 300% shear strain amplitude shown in Fig.1 superimposed with those predicted by the non-linear hysteresis model (- - -) with $K_1 = 0.9$ and $K_2 = 4.5$

The double shear testpiece used to generate the observed loops in Fig.1 was later subjected to a history involving reversals within the main loop. The waveform was scaled for each test so that the peak strain in the rubber was varied from 50% to 300%. The experimental and predicted hysteresis loops are shown in Fig.5 for peak strains in the rubber of 100 and 300%. The predicted behaviour agrees reasonably well with the observations, except that the observed damping within the subsidiary loops is underestimated by the model. The discrepancy suggests that some rate-dependent damping should be added to the model.

Bi-linear model

Three bi-linear models are chosen here to characterise the dynamic behaviour of HDNR at 100% strain amplitude. The parameters for the models are calculated such that their secant stiffness and loss factor at 100% equals that given by the non-linear hysteretic model described in the previous section. No attempt is made to optimize the parameters of the model over a range of strains. The loss factor can be calculated from (see Fig.6):

$$\sin\delta = \frac{4}{\pi m} \frac{(1-n)(m-1)}{(1-n+mn)} \quad (2)$$

where $n = K_2/K_1$ and $m = D/x_r$. Parameter n gives a measure of the degree of non-linearity of the model. The values for n were 0.225, 0.475 and 0.6.

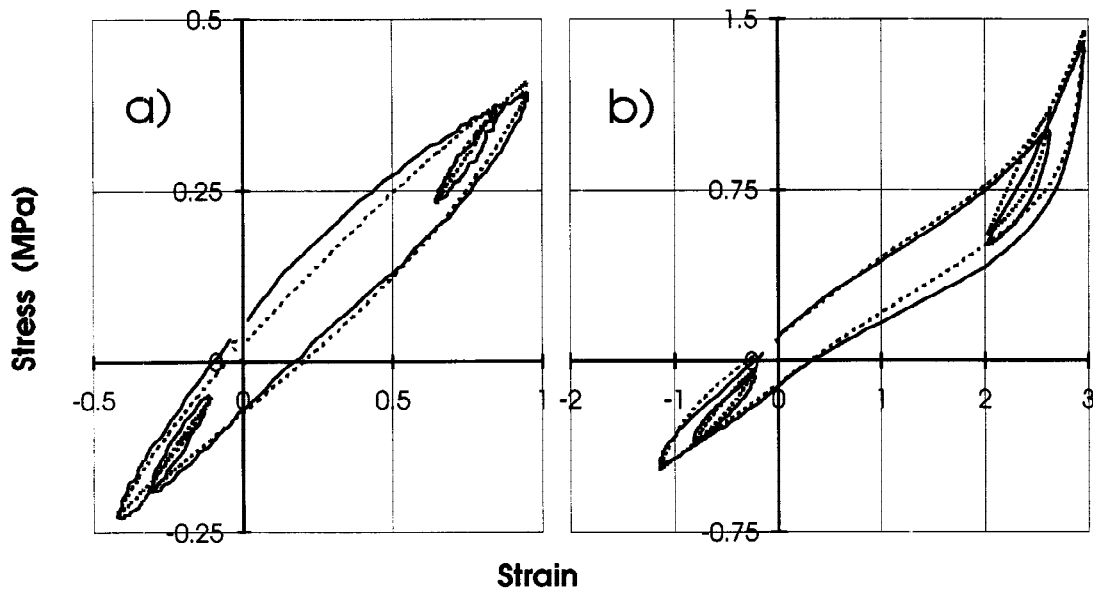


Fig.5 Experimental loops (—) and loops calculated using the non-linear hysteresis model for the HDNR (- - -). The testpiece was subjected to superimposed sinusoidal deformations. The peak shear strains in the HDNR were (a) 100% and (b) 300%

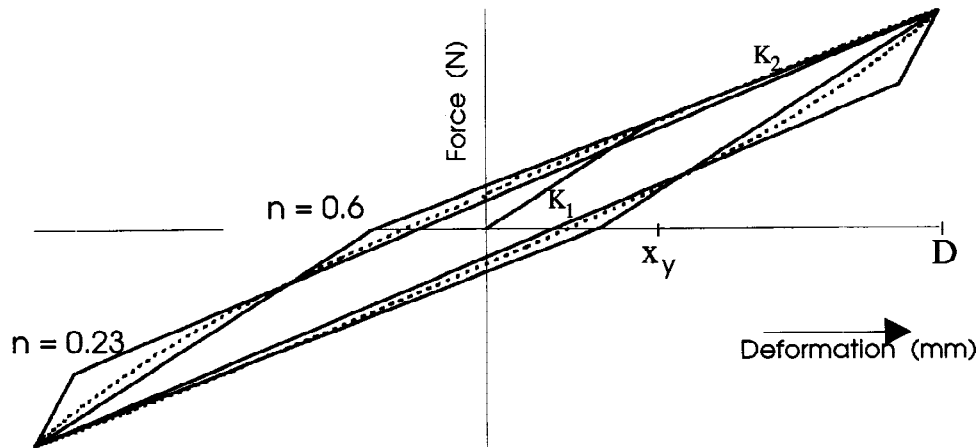


Fig.6 The 100% experimental loop (- - -) shown in Fig.1 approximated by two bi-linear models. Initial stiffness K_1 is only shown for the case of $n = 0.6$. $n = K_2/K_1$. x_y and D are the yield and 100% strain deflection

Linear models

Three possible methods of producing linearised parameters from the non-linear stress-strain data are discussed. The detailed description of each method is given by Ahmadi & Muhr (1995). Each method defines G_{dyn} and $\sin\delta$ in such a way that the area of the hysteresis loop (W_L) for the strain amplitude $\tilde{\gamma}$ is given by:-

$$W_L = \pi G_{dyn} \tilde{\gamma}^2 \sin\delta \quad (3)$$

The methods and corresponding definition of parameters are given in Table 1.

Table 1 Calculation of linearised parameters

Method	Secant	Harmonic	Skeleton
G_{dyn} $\sin\delta$	$\tau_{peak}/\bar{\gamma}$ eq.(3)	$\bar{\tau}_1/\bar{\gamma}$ eq.(3); $\delta = \delta_1$	$2W_s/\bar{\gamma}^2$ eq.(3)

τ_{peak} = peak stress; τ_1 = amplitude of first harmonic of stress response; δ_1 = phase angle for first harmonic of response; W_s = area under the skeleton curve constructed by taking the mean values of τ corresponding to increasing and decreasing γ from $\gamma = 0$ to $\gamma = \bar{\gamma}$.

APPLICATION OF MODELS TO A SOFT HIGH DAMPING NR VULCANIZATE

G_{dyn} and $\tan\delta$ results, calculated according to the three methods of linearization from hysteresis loops generated from a double shear testpiece of the soft HDNR vulcanizate, are given in Table 2 and Fig.12 of Ahmadi & Muhr (1995). The harmonic method gives intermediate values, with the secant method giving the highest G_{dyn} and the lowest $\tan\delta$. Figure 7 shows a comparison between the dynamic properties obtained from the experimental data, and the loops predicted by the non-linear hysteretic and bi-linear ($n = 0.6$) models; the parameters are calculated using the secant method.

The spectral response is predicted from three unscaled strong motion records using the non-linear hysteretic model, bi-linear models and the linear models. The results from two records are given in Table 2; the other one studied is the Pacoima record. Where necessary the secant method is used to specify the design parameters (such as total rubber thickness) of the isolation system such that a rubber strain of 100% is realised at the peak displacement response and a nominal isolation frequency of 0.5Hz is achieved for that displacement.

Table 2. Predicted peak responses to unscaled time-history records

		Non-linear model	Bi-linear models n			Linear models		
			0.23	0.48	0.6	Secant	Harmonic	Skeleton
G_{dyn} (100%)(MPa)		0.429	0.429	0.429	0.429	0.429	0.420	0.401
$\tan\delta$ (100%)		0.161	0.161	0.161	0.161	0.161	0.167	0.173
k/m (s^{-2})		9.87	9.87	9.87	9.87	9.87	9.66	9.23
c/m (s^{-1})		0.506	0.506	0.506	0.506	0.506	0.525	0.544
K_1		0.9	3.81×10^7	1.77×10^7	1.32×10^7	-	-	-
K_2		4.5	8.57×10^6	8.4×10^6	7.90×10^6	-	-	-
El Centro	S_A (ms^{-2})	1.51	1.31	1.29	1.47	1.60	1.60	1.62
D = 159.7	S_D (mm)	152.3	128.9	125.5	145.8	159.7	163.3	172.1
	x_y (mm)	-	6.96	25.1	59.5	-	-	-
	Parkfield	S_A (ms^{-2})	1.05	0.98	1.01	1.09	0.96	0.94
D = 95.3	S_D (mm)	109.7	99.9	103.7	114.9	95.3	94.5	93.3
	x_y (mm)	-	4.15	15.0	35.5	-	-	-

Note: strain at which rubber properties are defined = 100%; k = linearised stiffness (for non-linear and bi-linear models, secant stiffness); c = damping coefficient
 m = mass of system S_D = peak spectral displacement S_A = peak spectral acceleration

Table 3 illustrates the difference between spectral responses predicted using the non-linear hysteretic and linear models for earthquake inputs larger than the design level. The inputs are obtained by scaling the records of Table 2 by the factor λ . Three cases are reported: (a) $\lambda = 2.5$, the parameters for the linear models being those at $\gamma = 250\%$; (b) $\lambda = 2$; the parameters for the linear models are set according to the peak strain in the bearing (Ahmadi & Muhr 1993) using an iteration procedure; (c) for each earthquake input, λ is adjusted so that the peak bearing displacement is 250% based on the non-linear hysteretic model prediction, the linear model parameters being set at this strain.

Table 3. Predicted peak responses to severe time-history records

		Non-linear hysteretic model	Linear Models		
			Secant	Harmonic	Skeleton
(a) $\lambda = 2.5$ (Non-iterated)					
El Centro	S_A (ms^{-2})	5.45	4.26	4.30	4.21
	S_D (mm)	478.2	458.5	510.2	527.2
Parkfield	S_A (ms^{-2})	3.02	2.29	2.0	1.84
	S_D (mm)	277.8	245.1	236.1	230.4
(b) $\lambda = 2$ (Iterated)					
El Centro	S_A (ms^{-2})	3.07	3.42	3.44	3.37
	S_D (mm)	354.1	374.5	405	419.8
Parkfield	S_A (ms^{-2})	1.99	1.70	1.63	1.56
	S_D (mm)	225.2	192.6	189.7	187.5
(c) λ Variable					
El Centro	S_A (ms^{-2})	3.64	3.71	3.74	3.66
	S_D (mm)	399.5	399	444	459
Parkfield	S_A (ms^{-2})	2.18	1.94	1.69	1.56
	S_D (mm)	239	208	200	195

DISCUSSION AND CONCLUSIONS

The non-linear hysteretic model appears to predict the dynamic properties of the HDNR vulcanizate reasonably well from 50 to 300% shear strain amplitude (see Fig.7). The loops for the small strain amplitudes ($\gamma \leq 100\%$) and the subsidiary loops in Fig.5 suggest the presence of a rate-dependent mechanism for dissipating energy, though this may be small compared with the contribution to damping due to a "friction -type" process, ie. hysteretic damping. The harmonic content of the sinusoidal stress waveform predicted by the model compares very well to that of the experimental data. This is important in predicting the response of internal equipment in an isolated structure (Ahmadi *et al*, 1994). Results shown in Table 2 indicate that the bi-linear model with $n = 0.6$ (see Fig.6) agrees (within 5%) better with the non-linear model than those with $n = 0.23$ and 0.48 ; the last two, however, clearly followed the observed hysteresis loops less well. For this particular analysis therefore, modelling the curvature in the loading path by two linear elements (K_1 and K_2) can be adequate in predicting the peak responses of the isolation system, provided care is taken in the choice of n . The maximum spread between the predictions of the linear models is 12%. For a given earthquake ground motion, the linear models give predictions all above or all below that from the non-linear hysteretic model; they are conservative for the El Centro input. For the three inputs studied, the secant model always gives predictions closest (within 13%) to the non-linear model. For inputs much larger than the design level (see Table 3) the agreement between the responses predicted by the non-linear model and linear models is poorer, and the spread between them greater

(30%). Overall the secant method clearly gives predictions closest to those of the non-linear hysteretic model, though the discrepancies are up to for case (a) 24%, for (b) 17% and for (c) 12%. Iteration as in case (b) results in a linear prediction closer to that of the non-linear model than simply assuming the peak rubber strain scales linearly with the ground motion, but the approach of case (c) gives closer agreement.

For ground motions producing high strain amplitudes, a linear analysis, even for the moderately non-linear compound studied here, results in predictions not necessarily conservative and reliable to only about 25% according to the records studied here. The presence of high levels of harmonics is also indicative of inadequacies in the linear analysis (Ahmadi & Muhr, 1993). Nevertheless, at the design level earthquake a linear approach using the secant parameters may be considered adequate.

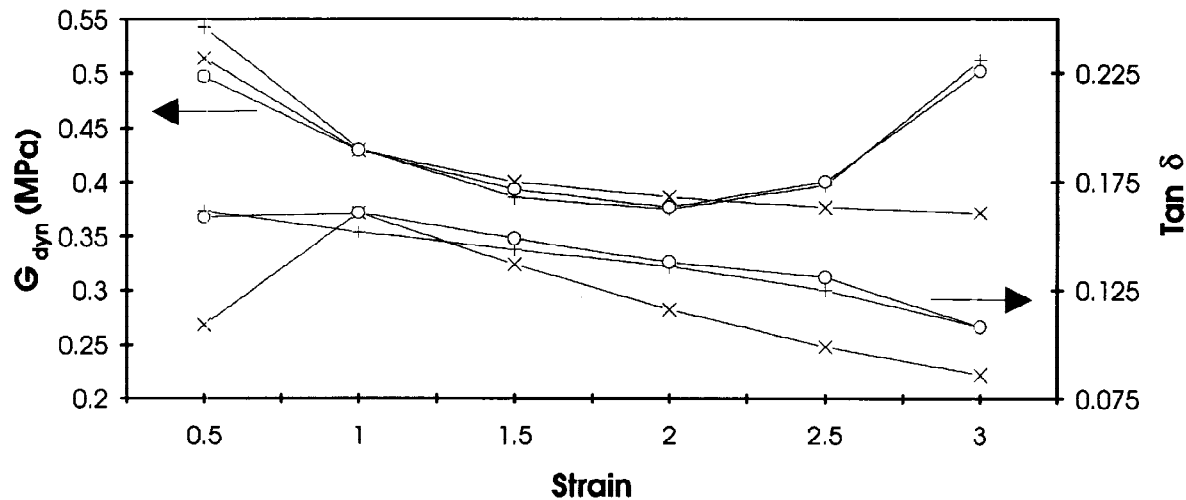


Fig.7 The dynamic shear modulus G_{dyn} and loss factor $\tan \delta$ as a function of strain amplitude. + experimental; x bi-linear ($n = 0.6$) and o non-linear hysteretic data ($K_1 = 0.9$, $K_2 = 4.5$). The parameters are obtained using secant method.

REFERENCES

- Ahmadi, H.R. and Muhr, A.H. (1995). Contribution of MRPPRA to development of design guidelines for isolated structures. International Post-SMiRT Conference Seminar on Seismic Isolation, Passive Energy Dissipation and Control of Vibrations of Structures. Santiago, Chile, August 21 to 23, 1995
- Ahmadi, H.R., Crawshaw, J. and Fuller, K.N.G. (1995). The influence of non-linearity on the response of rubber isolators to earthquake motions. Proceedings of the 10th European Conference on Earthquake Engineering, Vienna, Austria, 28th August - 2nd September 1995, 1, 677-682. Balkema, Rotterdam
- Fuller, K.N.G., Ahmadi, H.R. and Coveney, V.A. (1991). Seismic isolation with high damping rubber bearings theory and practice. In Earthquake, Blast and Impact - Measurement and effects of Vibration (SECED, ed.), pp.141-150. Elsevier Applied Science, London
- Skinner, R.I., Robinson, W.H. and McVerry, G.H. (1993). An Introduction to Seismic Isolation. John Wiley & Sons, Chichester

ACKNOWLEDGEMENT

The authors wish to thank Malcolm Phillips for preparing the computer codes, Niall Walsh for carrying out the numerical analysis and Susan Luck for typing this manuscript.